Lipids in Health and Disease

RESEARCH

Open Access

Free fatty acids may regulate the expression of 11β-hydroxysteroid dehydrogenase type 1 in the liver of high-fat diet golden hamsters through the ERS-CHOP-C/EBPα signaling pathway

Dandan Liu[1,2,3], Peipei Tian[1,2,4], Yilin Hou[1,2], Tingxue Zhang[1,2], Xiaoyu Hou[1,2], Lifang Liu[1,2,3], Xiaolong Li[1,2,5], Kunjie Zheng[1,2,5], Chao Wang[6] and Guangyao Song[1,2*]

Abstract

Objective Free fatty acids (FFA) can increase the expression of 11β-hydroxysteroid dehydrogenase 1 (11β-HSD1) in local tissues and organs. However, the mechanism underlying the effect of FFA on 11β-HSD1 expression remains unclear.

Methods A total of 24 male Syrian golden hamsters (SPF grade) were selected and randomly divided into a control group (Con, $n=8$) fed a normal diet, and a high-fat diet group ($n=16$) fed for 12 weeks. After successfully establishing the hyperlipidemia hamster model, the high-fat group was further divided into a high-fat group (HF) and a fenofibrate intervention group (Feno). Following an oral fat tolerance test (OFTT), blood lipids and FFA levels were measured. The expression levels of endoplasmic reticulum stress (ERS) marker GRP78, downstream key molecule CHOP, C/EBPα, and 11β-HSD1 were analyzed using Western blot and RT-PCR.

Results After OFTT, FFA levels in all three groups initially decreased and then increased, with the highest levels observed in the HF group (Ps < 0.05). FFA levels in the Feno group were comparable to those in the Con group ($P > 0.05$). Hepatic FFA, 11β-HSD1, and corticosterone levels were highest in the HF group (Ps < 0.05), while the Feno group showed no significant difference compared to the Con group (Ps > 0.05). Hepatic 11β-HSD1 and corticosterone levels were positively correlated with FFA levels (Ps < 0.05). Western blot and RT-PCR results indicated higher GRP78, CHOP, C/EBPα, and 11β-HSD1 protein and mRNA expression in the HF group compared to the Con group (Ps < 0.05). Fenofibrate intervention reduced FFA levels and downregulated these indicators in the Feno group compared to the HF group (Ps < 0.05).

Conclusion FFA may regulate the expression of hepatic 11β-HSD1 in high-fat-fed golden hamsters via the ERS-CHOP-C/EBPα signaling pathway, thereby affecting local corticosterone levels. Fenofibrate may downregulate the levels of 11β-HSD1 and corticosterone in local tissues by reducing FFA levels.

*Correspondence:
Guangyao Song
sguangyao2@163.com
Full list of author information is available at the end of the article

Keywords Free fatty acids, 11β-hydroxysteroid dehydrogenase 1, Endoplasmic reticulum stress, CCAAT/enhancer-binding protein homologous protein, CCAAT/enhancer-binding protein α, Corticosterone

Introduction

The release of glucocorticoids (GCs) in circulation is primarily regulated by the hypothalamic–pituitary–adrenal axis. Approximately 4% of circulating GCs exist in a free form with biological activity, while about 96% are bound to proteins and lack biological activity [1]. The cellular and tissue response to GCs depends largely on their local concentration, which is influenced by the expression of 11β-hydroxysteroid dehydrogenase 1 (11β-HSD1) [2].

11β-HSD1 is a metabolic enzyme of GCs that interconverts inactive and active forms. However, its primary function in vivo is to convert inactive GCs into their active form, thereby regulating their local concentration in tissues and acting as a local amplifier of GCs [3]. 11β-HSD1 is highly expressed in organs such as the liver, adipose tissue, and brain [4]. The local activity of 11β-HSD1 in tissues is a major determinant of the adverse metabolic outcomes caused by excess circulating GCs, contributing to the development of metabolic syndrome [2].

GCs play a crucial and complex role in various lipid metabolic pathways [5]. Elevated levels of GCs can lead to dyslipidemia [6]. Does lipid metabolism disorder, in turn, influence GC levels? A study by Petrus P et al. on biopsy samples from 45 obese women revealed that local saturated fatty acids were associated with increased expression of the 11β-HSD1 gene and protein in visceral adipose tissue [7]. Similarly, Vara Prasad SS et al. demonstrated that dietary trans and saturated fatty acids upregulated 11β-HSD1 expression in retroperitoneal white adipose tissue of rats, enhancing the local effects of GCs. They also found that CCAAT/enhancer-binding protein α (C/EBPα), a known transcriptional activator of 11β-HSD1, had increased mRNA expression in the adipose tissue of rats fed diets rich in trans and saturated fatty acids [8].

The endoplasmic reticulum (ER) is an organelle responsible for protein folding, maturation, quality control, and transport. The primary nutrients that harm cells by affecting the ER are FFAs and glucose, with the harmful effects of FFAs likely related to their excessive incorporation into membrane structures [9]. The most common saturated FFA, palmitate (PA), induces ER stress (ERS) in various peripheral tissues and cells, with prolonged ERS and increased levels leading to the expression and activation of glucose-regulated protein 78 (GRP78) and C/EBP homologous protein (CHOP), further causing cellular dysfunction and even apoptosis [10–14]. CCAAT/enhancer-binding proteins (C/EBP) are a family of transcription factors with a conserved leucine zipper (bZIP) domain that dimerize and bind to DNA through a nearby basic region [15]. C/EBPα is highly expressed in adipocytes, hepatocytes, type II alveolar epithelial cells, and myeloid cells in the hematopoietic system, mainly functioning as a transcription factor to regulate adipogenesis, lipid metabolism in hepatocytes, lung development, bone marrow formation, and differentiation [16]. CHOP, also known as C/EBPζ, is a member of the C/EBP family that lacks the bZIP motif and shows low homology with other C/EBP family members. It is a key downstream molecule of ERS. Upon activation, CHOP can bind with C/EBPα and enter the nucleus, affecting ER function and cell vitality by influencing target genes involved in protein synthesis and oxidative protein folding. Prolonged activation of CHOP is considered a critical trigger for ERS-related apoptosis [17–19].

Peroxisome proliferator-activated receptor α (PPARα) is a major regulator of hepatic lipid metabolism and is involved in many pathophysiological processes induced by GCs, including gluconeogenesis, ketogenesis, insulin resistance, hypertension, and anti-inflammatory effects [20, 21]. FFA serve as ligands for PPARα, and fenofibrate, a PPARα agonist, is one of the most commonly used drugs to treat hypertriglyceridemia. In summary, this study aims to establish a hyperlipidemic golden hamster model by feeding a high-fat diet and observe the levels of corticosterone, 11β-HSD1, and FFA in the liver of hyperlipidemic golden hamsters and their interrelationships. After fenofibrate intervention in hyperlipidemic golden hamsters, FFA levels will decrease, and changes in hepatic corticosterone and 11β-HSD1 levels will be observed. The study will analyze whether FFA regulate the expression of 11β-HSD1 in the liver of high-fat diet golden hamsters through the ERS-CHOP-C/EBPα signaling pathway.

Materials and methods

Experimental animals

A total of 24 male Syrian golden hamsters (SPF grade), 8 weeks old and weighing 100–150 g, were purchased from Hebei Yiweivo Biotechnology Co., Ltd. (Production license number: SCXK (Hebei) 2020–002). The study was conducted in strict compliance with international animal management guidelines and approved by the Ethics Committee of Hebei General Hospital (Approval No. 202226).

The animals were housed in pairs in a barrier system at the Key Laboratory for Metabolic Diseases, Hebei Province, with a temperature of 21–25 °C, relative humidity of 50%, and a 12-h light–dark cycle. They had free access to food and water, with regular feed, water replacement, and cage cleaning. Diets were provided by Spefo (Beijing) Biotechnology Co., Ltd. The normal diet (D12450J) consisted of 70% carbohydrates, 20% protein, and 10% fat, providing 3.85 kcal/g. The high-fat diet (D12492) had 20% protein, 20% carbohydrates, and 60% fat [22], providing 5.24 kcal/g.

All hamsters were acclimatized for one week before the experiment, during which their activity, eating behavior, and growth were normal.

Animal grouping and experimental protocol

From the 24 golden hamsters, 8 were randomly selected as the Control group (Con) and fed with a standard diet. The remaining 16 hamsters were assigned to the High-fat diet group (HF) and fed with a high-fat diet. The feeding continued for 12 weeks, after which lipid metabolism was evaluated in all hamsters at the end of week 12 to confirm the successful establishment of a hyperlipidemia model.

Once the hyperlipidemia model was successfully established, the 16 HF hamsters continued on a high-fat diet. Among them, 8 hamsters were randomly assigned to the Fenofibrate intervention group (Feno) and administered fenofibrate suspension daily by gavage. The suspension was prepared by dissolving 200 mg of fenofibrate in 40 mL of 0.1% DMSO saline solution, resulting in a 5 mg/mL fenofibrate solution. The dosage was 50 mg/kg body weight [23–26]. The remaining 8 hamsters were maintained as the High-fat control group (HF). The Con group of 8 hamsters continued on a standard diet. Both the Con and HF groups received daily gavage with an equivalent volume of 0.1% DMSO saline solution, matching the volume given to the Feno group. The three groups were maintained under these feeding and intervention conditions for another 12 weeks.

For dissection, 2% sodium pentobarbital injection (45 mg per 100 g body weight) was used for intraperitoneal anesthesia. Blood samples were collected from the abdominal aorta, and liver tissues were separated. Throughout the study, measures were taken to minimize animal discomfort and suffering.

Oral Fat Tolerance Test (OFTT)

At the end of week 24, all hamsters underwent the OFTT [27]. The animals were fasted overnight for 12 h with access to water. At the start of the test, body weight was recorded, and olive oil was administered orally at a dose of 450 μL per 100 g body weight. Blood samples were collected from the retro-orbital venous plexus at 0, 0.5, 1, 2, 3, and 4 h post-gavage to measure FFA, Total Cholesterol (TC), Triglycerides (TG), High-Density Lipoprotein Cholesterol (HDL-C), and Low-Density Lipoprotein Cholesterol (LDL-C).

Biochemical indicator measurement

FFA was measured using an enzyme method (Jiancheng Bioengineering Institute, Nanjing, China). TC was measured by the COD-PAP method (Jiancheng Bioengineering Institute, Nanjing, China), TG were measured by the GPO-PAP method (Jiancheng Bioengineering Institute, Nanjing, China), HDL-C and LDL-C were measured by the direct two-reagent method (Jiancheng Bioengineering Institute, Nanjing, China). Corticosterone and 11β-HSD1 were measured using competitive inhibition enzyme-linked immunosorbent assays (ELISA) (Yunclone Technology Co., Ltd., Wuhan, China). All of these indicators were determined using an automated microplate reader (VERSAmax, USA). Liver tissue was homogenized using an ultrasonic disruptor, and the supernatant was collected for BCA protein concentration determination before measuring the relevant indicators.

Western blot

Liver tissue from the golden hamsters was ground using an automatic sample freeze grinder, followed by complete lysis. Protein concentration was measured using the BCA method (Abbkine). SDS-PAGE gel was prepared using a one-step SDS-PAGE gel kit (Biotides). After adding Marker (Mei5bio) and protein samples into the wells, electrophoresis was carried out. Following electrophoresis, membrane transfer was performed. The PVDF membrane was incubated in a quick blocking solution for blocking. The primary antibody (Beyotime) was diluted according to the recommended ratio, and after blocking (Beyotime), the PVDF membrane was cut according to the molecular weight of different proteins, placed into incubation boxes with the corresponding primary antibody, and incubated overnight at 4 °C. After washing, the membrane was incubated with horseradish peroxidase-conjugated secondary antibody at room temperature for 1 h. Enhanced chemiluminescence (ECL) was used for detection. The grayscale values of the bands were read using ImageJ software. The expression level of each target protein was calculated as the ratio of the grayscale value of the band to the corresponding β-actin grayscale value. Statistical analysis and graphing of the expression levels of each target protein were then performed.

Antibodies were purchased from: ZenBio-β-actin (380,624, 1:10,000); ZenBio-PPARα (340,843, 1:1000); Abcam-GRP78 (AB21685, 1:1000); Abcam-DDIT3 (CHOP) (AB317378, 1:2000); Abcam-CEBP Alpha (AB40764, 1:1000); Abcam-HSD11B1 (AB39364, 1:1000).

Reverse Transcription-Polymerase Chain Reaction (RT-PCR)

Approximately 50 mg of golden hamster liver tissue was used to extract total RNA using a total RNA extraction kit (TianGen Biochemical Technology Beijing Co., Ltd., China). RNA content and purity were measured using a NanoDrop 2000, with an OD260/OD280 ratio between 1.8–2.0, indicating the RNA was suitable for further reverse transcription. RNA was reverse transcribed into cDNA using the FastKing cDNA First-Strand Synthesis Kit (TianGen Biochemical Technology Beijing Co., Ltd., China), incubated at 42 °C for 15 min and 95 °C for 3 min. Using cDNA as a template, primers were combined with SuperReal fluorescent quantitative PCR premix reagent (TianGen Biochemical Technology Beijing Co., Ltd., China) for PCR amplification. After the Real-time PCR reaction, results were analyzed using ABI 7500 software, with β-actin as the internal reference gene. The CT values of different gene amplifications for each group were calculated. The relative quantification (RQ) value of the target gene for each group was determined using the formula RQ = 2^(-ΔΔCT), and statistical analysis was then performed.

Primer sequences

β-actin *F*-ATATCGCTGCGCTCGTTGTC, *R*-CACCCACGTACGAGTCCTTC; PPARα *F*-TGGGATGTCACACAATGCGA, *R*-AGGTAGGCCTCGTGGATTCT; GRP78 *F*-TCGGTGGGTCTACTCGGATT, *R*-AGAGGACACACGTCAAGCAG;DDIT3 (CHOP) *F*-AGTCCCTGCCATTCACCTTG, *R*-TTTCATCCGAGGACAGCACC; CEBP Alpha *F*-GCGAACACGAGACGTCCATA, *R*-AGGAACTCGTCGTTGAAGGC; HSD11B1 *F*-CATCTGCCCACTACATCGCT, *R*-ATTGCTCCGCGAACGTCATA。

Statistical methods

Data were analyzed using SPSS 27.0 software. For normally distributed continuous data, values are presented as mean ± standard deviation ($\bar{x} \pm s$), and for non-normally distributed continuous data, as median and interquartile range (IQR). If the data were normally distributed with equal variances, an independent sample t-test was used for comparisons between two groups, and one-way analysis of variance (ANOVA) was used for comparisons between three groups. Repeated measures ANOVA was used to compare differences in the same indicator at different time points; otherwise, non-parametric tests were employed. If differences between three groups were statistically significant, pairwise comparisons were performed. For linear correlation analysis of two variables, Pearson correlation was used if the data were normally distributed with equal variances, otherwise Spearman rank correlation was applied. A p-value of < 0.05 was considered statistically significant. Graphs were created using GraphPad Prism 9 software.

Results

Comparison of indicators between two groups of golden hamsters during the establishment phase of hyperlipidemic golden hamster model

Daily average caloric intake and weight changes of golden hamsters in the hyperlipidemic model establishment phase

During the establishment phase of the hyperlipidemic golden hamster model, as the hamsters continued to grow, their food intake gradually increased. The daily average caloric intake was recorded every two weeks, and there were no statistically significant differences between the two groups (Ps > 0.05, see Fig. 1A). At the beginning of the model establishment phase, there was no statistical difference in body weight between the Con group and HF group ($P > 0.05$). Subsequently, the body weight of the two groups gradually increased, and from the second

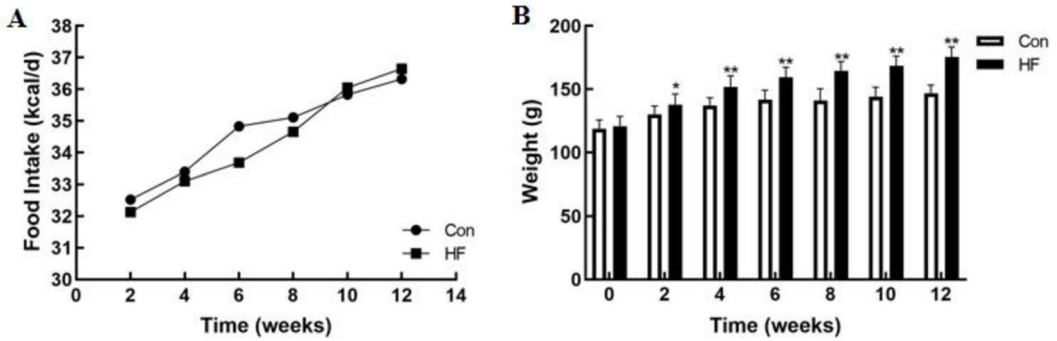

Fig. 1 The changes of daily average calories and body weight of golden hamsters with hyperlipidemia in the two groups during the establishment of the model. Figure **A** represents Average daily calorie intake and Figure **B** represents Weight change. There were 8 golden hamsters in the Con group and 16 in the HF group. *P<0.05 versus the Con group; **P≤0.001 versus the Con group.

week onward, the body weight of the HF group was significantly higher than that of the Con group, with a statistically significant difference (Ps < 0.05, see Fig. 1B).

Lipid metabolism of the two groups of golden hamsters during the establishment phase of the hyperlipidemia model

At the beginning of the hyperlipidemia model establishment phase, there were no significant differences in TC, TG, FFA, HDL-C, and LDL-C levels between the Con group and the HF group (Ps > 0.05). After 12 weeks of high-fat diet feeding, the TC, TG, FFA, HDL-C, and LDL-C levels in the HF group significantly increased and were notably higher than those in the Con group, with differences being statistically significant (Ps < 0.05, see Fig. 2). The results suggest that the hyperlipidemic golden hamster model was successfully established through high-fat diet feeding.

Comparison of indicators among the three groups of golden hamsters during the fenofibrate intervention phase

Changes in daily average caloric intake and body weight of golden hamsters in the fenofibrate intervention phase

During the 12-week fenofibrate intervention phase, there were no statistically significant differences in the daily average caloric intake among the three groups of golden hamsters (Ps > 0.05, see Fig. 3A). At any time point during the intervention phase, the body weight of golden hamsters in the HF group and Feno group was significantly higher than that in the Con group (Ps < 0.05, see Fig. 3B). The body weight of golden hamsters in the Feno group started to be slightly lower than that in the HF group from week 14, but the difference between the two groups was not statistically significant (Ps > 0.05, see Fig. 3B).

Liver H&E staining of the three groups of golden hamsters in the fenofibrate intervention stage

The liver cells of the Con group golden hamsters exhibited intact structure, with evenly distributed cytoplasm and no visible lipid vacuoles. The hepatic cords and sinusoids were arranged in a regular radiating pattern. In the HF group, the liver cells varied in size, and multiple lipid vacuoles were observed in the cytoplasm. The hepatic cords and sinusoids were disordered. In the Feno group, the liver cell structure was improved compared to the HF group, with a noticeable reduction in lipid vacuoles in the cytoplasm, and the arrangement of hepatic cords and sinusoids was improved (see Fig. 4).

Lipid metabolism of golden hamsters in the three groups in the fenofibrate intervention stage

Changes in blood lipids after OFTT in the three groups of golden hamsters At the end of week 24, the three groups

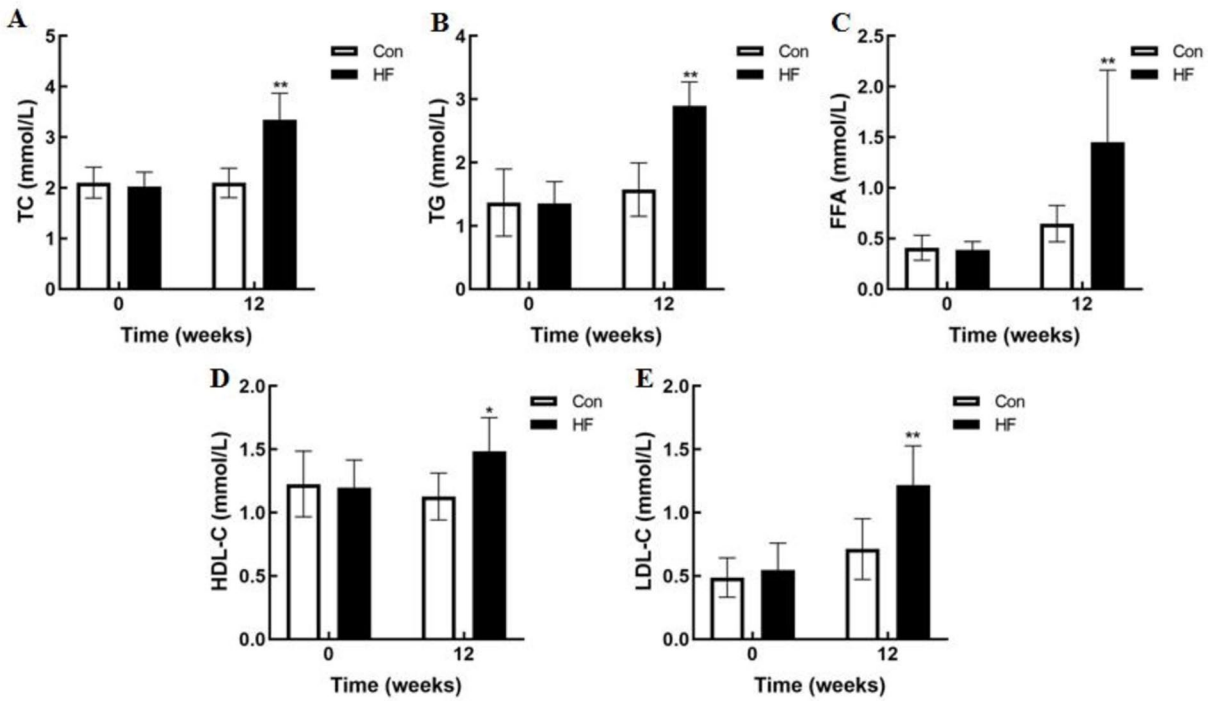

Fig. 2 Lipid metabolism of golden hamster with hyperlipidemia in two groups at the stage of model establishment. *$P < 0.05$ versus the Con group; **$P \leq 0.001$ versus the Con group

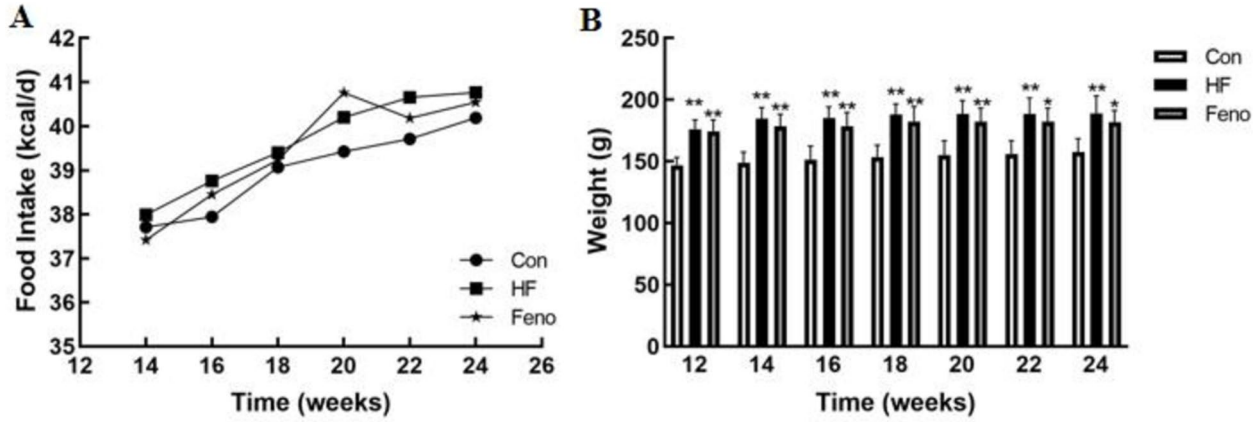

Fig. 3 The daily average calorie intake and body weight change of the three groups of golden hamsters in the fenofibrate intervention stage. Figure **A** represents Average daily calorie intake and Figure **B** represents Weight change. Each group has eight golden hamsters. *P<0.05 versus the Con group; **P≤0.001 versus the Con group; #P<0.05 versus the HF group; ##P≤0.001 versus the HF group.

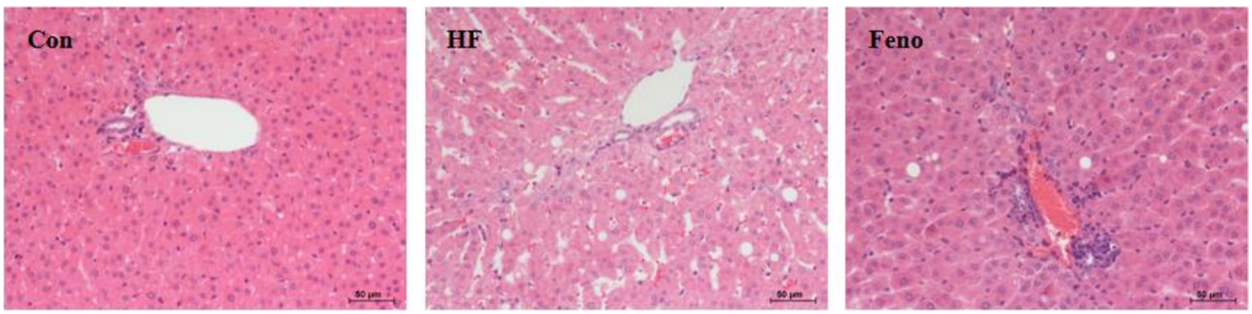

Fig. 4 Liver Tissue H&E Staining of the Three Groups of Golden Hamsters

of golden hamsters underwent the OFTT, and the results are shown in Fig. 5. Based on the blood lipid levels at 0 h, it can be observed that the TC, TG, HDL-C, and LDL-C levels in the HF group were higher than those in the Con group. After fenofibrate intervention, the TC, TG, and LDL-C levels in the Feno group were significantly lower than those in the HF group, while the HDL-C level was higher in the Feno group than in the HF group.

After OFTT, the TG levels showed significant changes across the three groups, while TC, HDL-C, and LDL-C levels showed little variation. In the Con group, the TG level peaked at 2 h post-OFTT and returned to fasting levels by 4 h. In the HF group, the TG level continued to rise up to 4 h post-OFTT. In the Feno group, the TG level peaked at 3 h post-OFTT and decreased at 4 h, though it remained higher than the fasting level.

Changes in FFA levels after OFTT in the three groups of golden hamsters After the OFTT, the FFA levels in all three groups of hamsters initially decreased and then increased. The FFA levels reached their lowest point 1 h post-meal and were above baseline levels 4 h after the meal (Ps < 0.05, see Fig. 6).

The FFA levels in the HF group were higher than those in the Con group at fasting and at 0.5 h, 1 h, 2 h, 3 h, and 4 h post-OFTT. Additionally, the FFA levels in the HF group were higher than those in the Feno group at fasting and at 0.5 h, 1 h, 3 h, and 4 h post-OFTT (Ps < 0.05). There were no statistically significant differences in FFA levels between the Con group and the Feno group at fasting and at 0.5 h, 1 h, 2 h, 3 h, and 4 h post-OFTT (Ps > 0.05, see Fig. 6).

Comparison of 11β-HSD1, corticosterone, and FFA levels in the livers of the three groups of golden hamsters and their correlations

Comparison of 11β-HSD1, corticosterone, and FFA levels in the livers of the three groups of golden hamsters

The HF group exhibited the highest liver 11β-HSD1 levels, with significant differences compared to both the

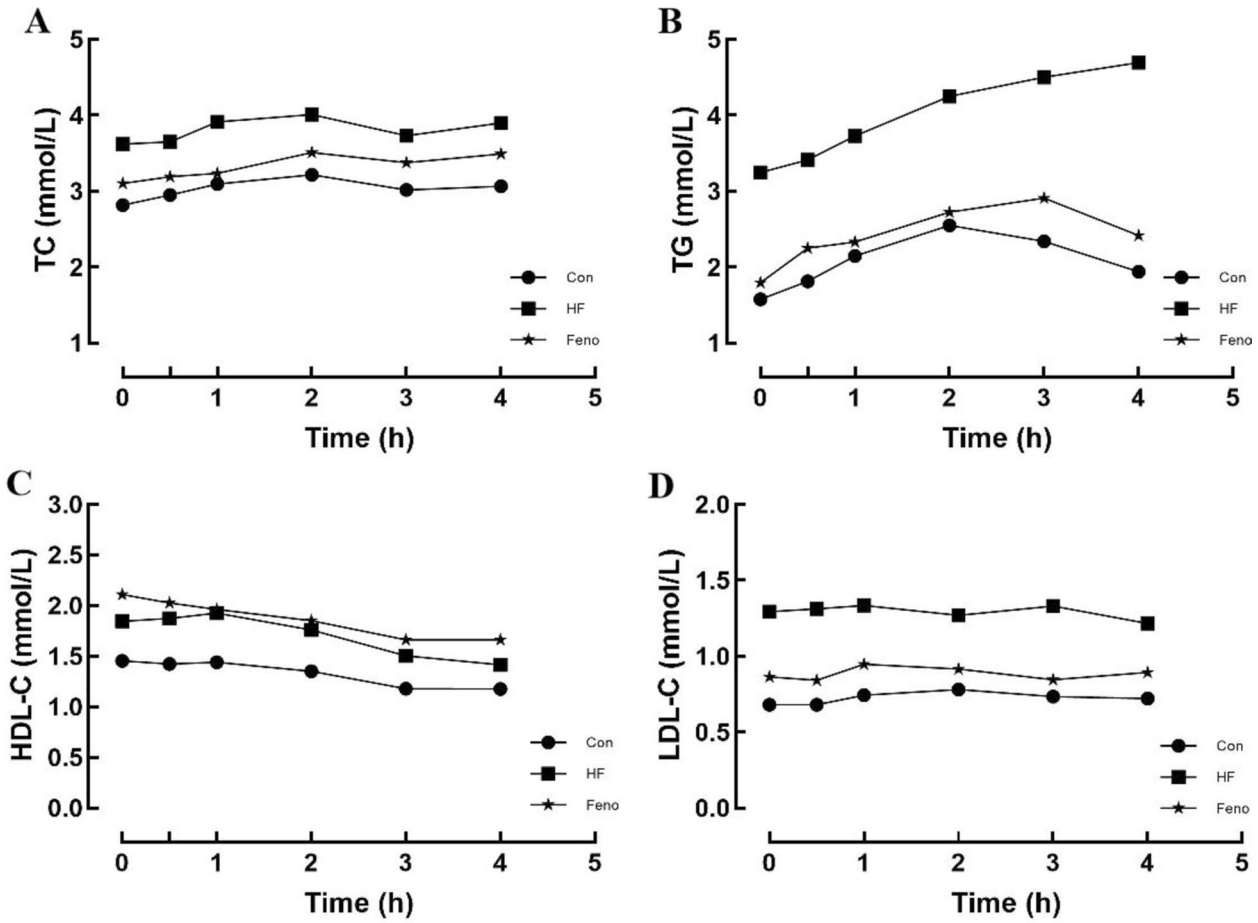

Fig. 5 Results of blood lipid after OFTT in three groups of golden hamster

Con and Feno groups (Ps < 0.05). There were no significant differences in liver 11β-HSD1 levels between the Con and Feno groups ($P > 0.05$). The HF group also had the highest corticosterone levels in the liver (Ps < 0.05), while there were no significant differences in corticosterone levels between the Con and Feno groups ($P > 0.05$). Additionally, the HF group showed the highest liver FFA levels (Ps ≤ 0.001), with no significant differences in liver FFA levels between the Con and Feno groups ($P > 0.05$) (see Fig. 7).

Correlation of liver 11β-HSD1, corticosterone, and FFA levels in the three groups of golden hamsters

Correlation analysis revealed significant positive correlations between liver 11β-HSD1 and corticosterone levels (r = 0.436, $P = 0.033$). There was also a significant positive correlation between liver 11β-HSD1 and FFA levels (r = 0.624, $P = 0.001$). Additionally, liver corticosterone levels were positively correlated with FFA levels (r = 0.532, $P = 0.007$) Fig. 8.

Changes in Liver PPARα, ERS-CHOP-C/EBPα signaling pathway proteins, and 11β-HSD1 protein expression in high-fat diet-fed golden hamsters and the effect of fenofibrate intervention

Changes in liver PPARα protein expression in the three groups of golden hamsters

Western blot results indicated that the liver PPARα protein expression level in the HF group was higher than that in the Con group, although the difference was not statistically significant ($P > 0.05$). However, the PPARα protein expression level in the Feno group, after Fenofibrate intervention, was significantly higher than that in both the HF and Con groups, with a statistically significant difference ($P < 0.05$, as shown in Fig. 9).

Changes in Liver ERS-CHOP-C/EBPα signaling pathway proteins and 11β-HSD1 protein expression in high-fat diet-fed golden hamsters and the effect of fenofibrate intervention

Western blot results indicated that the expression of GRP78, CHOP, and C/EBPα proteins in the liver tissue

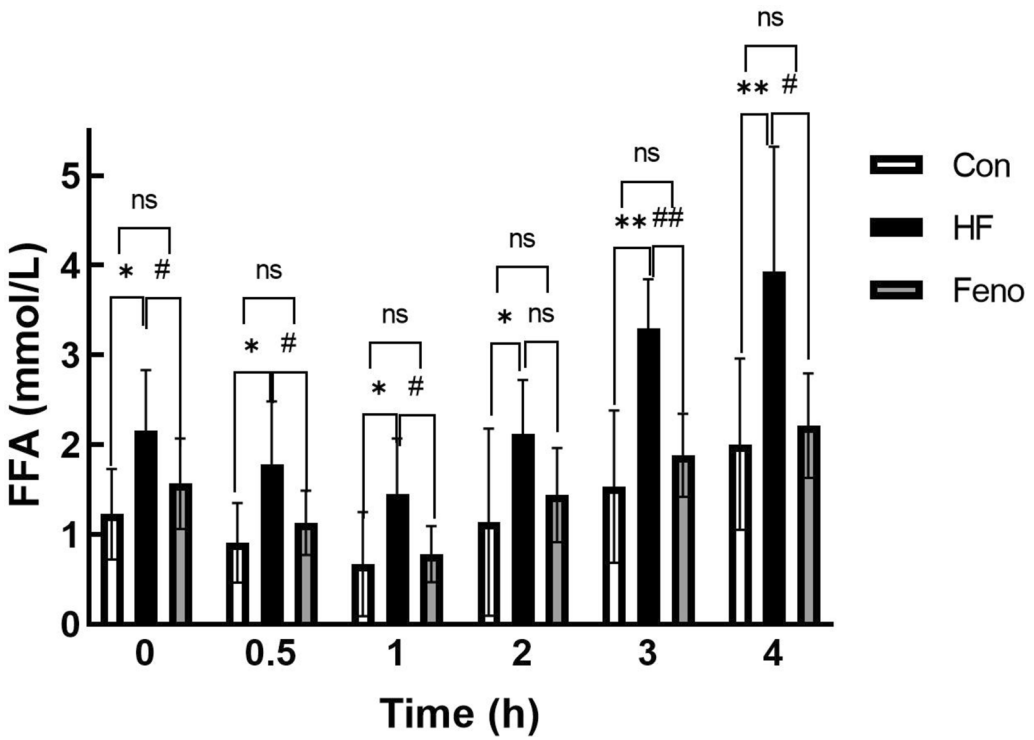

Fig. 6 FFA results after OFTT of golden hamster in three groups. *$P < 0.05$ versus the Con group; **$P \leq 0.001$ versus the Con group; #P < 0.05 versus the HF group; ##$P \leq 0.001$ versus the HF group; ns $P \geq 0.05$

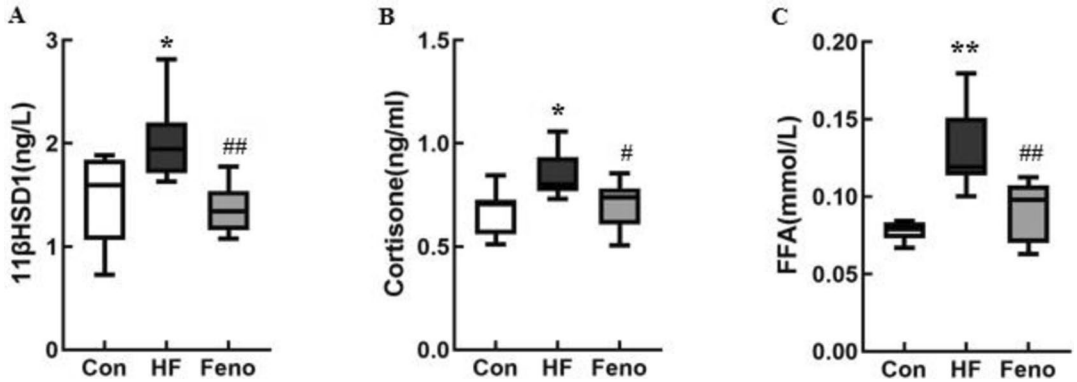

Fig. 7 Comparison of liver 11β-HSD1, corticosterone and FFA levels in three groups of golden hamsters. *$P < 0.05$ versus the Con group; **$P \leq 0.001$ versus the Con group; #$P < 0.05$ versus the HF group; ##$P \leq 0.001$ versus the HF group

of the HF group was significantly higher than that of the Con group, and the expression of 11β-HSD1 protein was also increased (P < 0.05). Fenofibrate intervention in the Feno group significantly reduced the expression of GRP78, CHOP, and C/EBPα proteins, and the expression of 11β-HSD1 protein decreased correspondingly ($P < 0.05$, as shown in Fig. 10). These protein expression results suggest that Fenofibrate can inhibit the ERS-CHOP-C/EBPα signaling pathway, thereby reducing the expression of 11β-HSD1 protein.

Changes in mRNA expression of PPARα, ERS-CHOP-C/EBPα signaling pathway, and 11β-HSD1 in the livers of high-fat diet-fed golden hamsters and the effect of fenofibrate intervention

RT-PCR results showed that, compared to the Con group, the mRNA expression of PPARα in the liver tissue of the HF group was higher, but the difference was not statistically significant ($P > 0.05$). Fenofibrate intervention in the Feno group significantly increased PPARα mRNA expression compared to both the HF

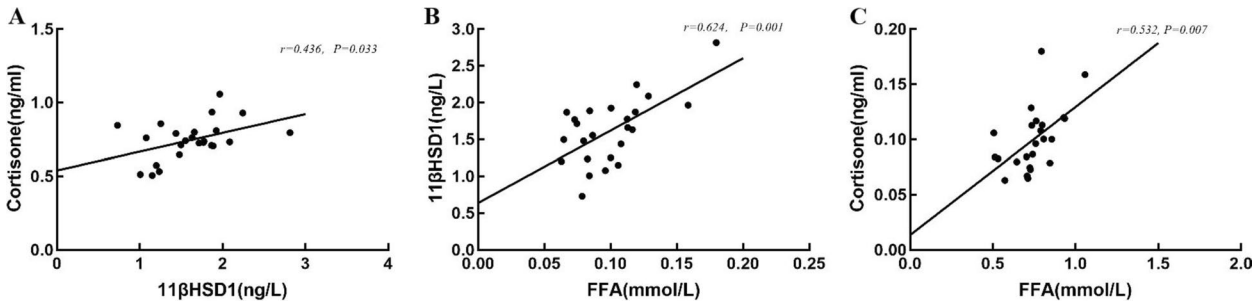

Fig. 8 Correlation of liver 11β-HSD1, cortisone and FFA levels in three groups of golden hamsters

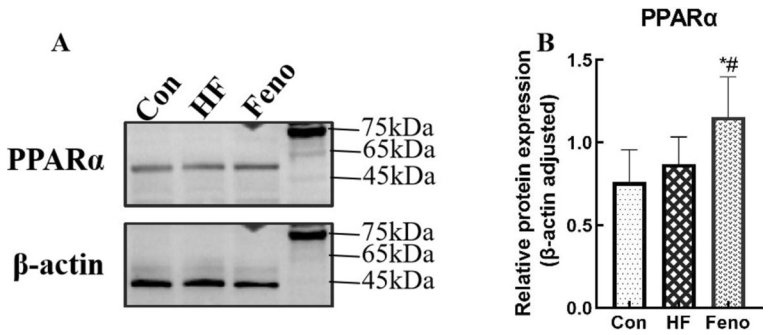

Fig. 9 Changes of liver PPARα protein expression in three groups of golden hamsters. *$P < 0.05$ versus the Con group; **$P \leq 0.001$ versus the Con group; #$P < 0.05$ versus the HF group; ##$P \leq 0.001$ versus the HF group

and Con groups ($P < 0.05$). In the HF group, the mRNA expression of GRP78, CHOP, and C/EBPα in the liver tissue was significantly higher than in the Con group, and the mRNA expression of 11β-HSD1 was also elevated ($P < 0.05$). Fenofibrate intervention significantly reduced the mRNA expression of GRP78, CHOP, and C/EBPα in the Feno group, and the expression of 11β-HSD1 mRNA decreased accordingly, with statistically significant differences ($P < 0.05$, as shown in Fig. 11). From the perspective of mRNA expression, fenofibrate can inhibit ERS-CHOP-C/ EBP-α signaling pathway, thereby reducing the expression of 11β-HSD1 mRNA.

Discussion

This study analyzed data from three groups of golden hamsters and found that a high-fat diet resulted in the highest levels of liver FFA, 11β-HSD1, and cortisol in the HF group. Fenofibrate intervention was able to reduce the elevation of these indicators caused by the high-fat diet. Significant positive correlations were observed between liver 11β-HSD1 and cortisol levels, 11β-HSD1 and FFA levels, and cortisol and FFA levels, suggesting that FFA levels may influence 11β-HSD1 expression, which in turn affects the local tissue cortisol levels. Both Western blot and RT-PCR results confirmed that high-fat feeding increased FFA levels in the liver, which may enhance ERS and increase the expression of ERS markers GRP78 and CHOP, promoting the translation of C/EBPα in liver cells. This ultimately resulted in increased 11β-HSD1 expression and elevated cortisol levels. These findings suggest that FFA might regulate 11β-HSD1 expression in the liver through the ERS-CHOP-C/EBPα signaling pathway. Fenofibrate intervention increased PPARα levels in the liver, reduced FFA levels, and decreased the expression of ERS-CHOP-C/EBPα signaling pathway proteins, leading to a decrease in 11β-HSD1 expression and lower cortisol levels. This further supports the idea that FFA may regulate 11β-HSD1 expression via the ERS-CHOP-C/EBPα signaling pathway.

11β-HSD1, located on the endoplasmic reticulum membrane, plays a crucial role in regulating local cortisol concentrations, which is independent of plasma cortisol levels. For example, feeding can trigger 11β-HSD1

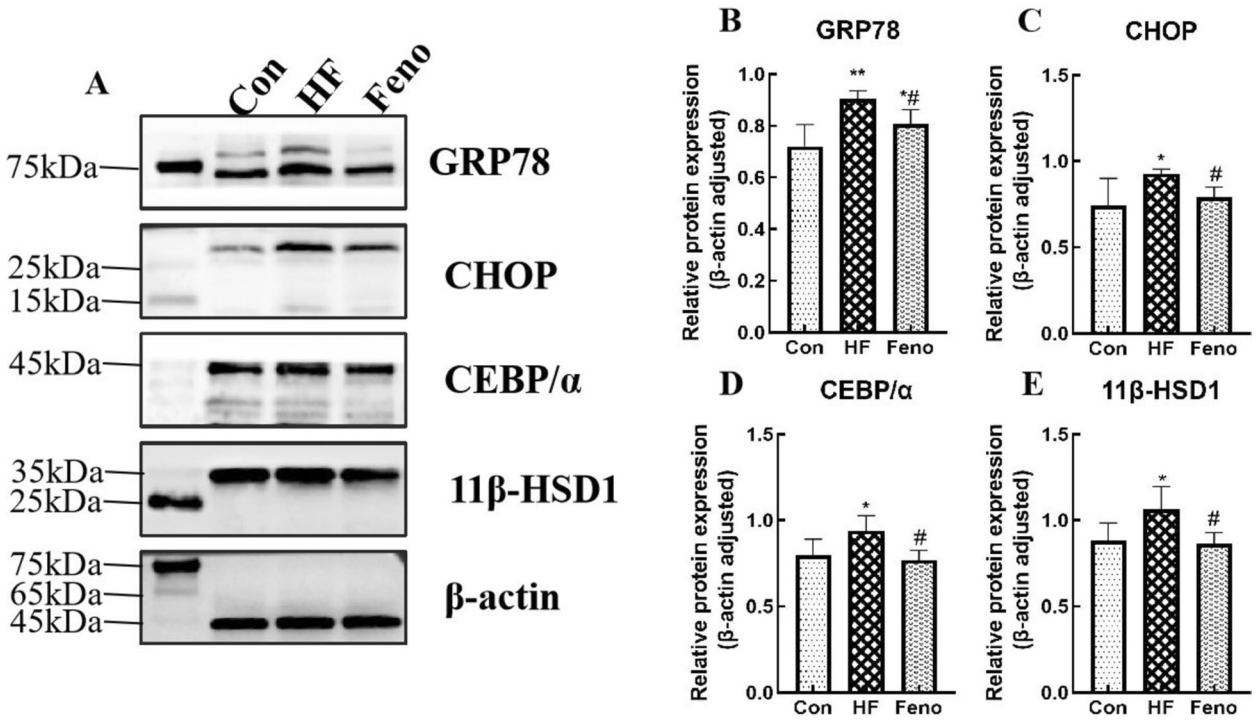

Fig. 10 Changes in the expression levels of ERS-CHOP-C/ EBP-α signaling pathway protein and 11β-HSD1 protein in the liver of golden hamsters fed a high-fat diet and the effects of fenofibrate intervention. **P* < 0.05 versus the Con group; ***P* ≤ 0.001 versus the Con group; #*P* < 0.05 versus the HF group; ##*P* ≤ 0.001 versus the HF group

to regulate local cortisol concentrations, making it a key component in adapting to changes in nutrient intake [28]. Research by Basu et al. indicated that when healthy male adrenal glands secrete approximately 38 nmol/min of cortisol, peripheral regeneration via 11β-HSD1 produces about 11 nmol/min [29]. Overfeeding in male rats after birth leads to upregulation of 11β-HSD1 expression in the liver [30]. Lipid infusion increased non-esterified fatty acids in the plasma of healthy cats by 1.7 times, leading to increased 11β-HSD1 expression in visceral and subcutaneous fat tissues and elevated local tissue glucocorticoid concentrations [31]. This study's findings suggest that high-fat diets elevate liver FFA, 11β-HSD1, and cortisol levels in the HF group. The significant positive correlations between liver 11β-HSD1 and cortisol levels, 11β-HSD1 and FFA levels, and cortisol and FFA levels suggest that FFA levels influence 11β-HSD1 expression in the hamster liver, further affecting the local cortisol concentrations.

Iwasaki Y et al. proposed that factors such as FFAs, insulin, and high-fat diets synergistically increase the expression of 11β-HSD1, leading to elevated cortisol levels in liver cells. This "intracellular Cushing's syndrome" in the liver underscores the molecular mechanisms behind the accumulation of metabolic syndrome risk, ultimately resulting in metabolic disorders [32]. 11β-HSD1 inhibitors (BVT.2733) can reduce 11β-HSD1 levels in mice, lowering local cortisol levels in tissues and preventing the onset of metabolic diseases induced by high-fat diets [33]. However, the exact mechanism by which FFAs influence 11β-HSD1 expression remains unclear and requires further research to clarify, providing new therapeutic targets for the prevention and treatment of metabolic diseases.

GRP78 is one of the most characteristic markers of ERS [34]. Activated GRP78 acts as a chaperone protein to enhance the protein-folding capacity of the ER, reducing the load of unfolded proteins within the ER [35]. ERS signaling promotes the formation of heterodimer complexes between CHOP and C/EBPα, which is essential for enhancing their action [36]. Physiological ERS is induced by food intake, and high-fat diets significantly exacerbate ERS, promoting the translation of key metabolic regulators C/EBPα and C/EBPβ, which indirectly regulate the expression of metabolic genes, further leading to disturbances in glucose and lipid metabolism [37, 38].

In 2000, Williams LJ et al. proposed that members of the C/EBP transcription factor family directly regulate the transcription of 11β-HSD1. The 11β-HSD1 promoter contains 10 C/EBP binding sites, one of which includes the transcription start site. Both C/EBPα and C/EBPβ are present in complexes formed by liver nuclear

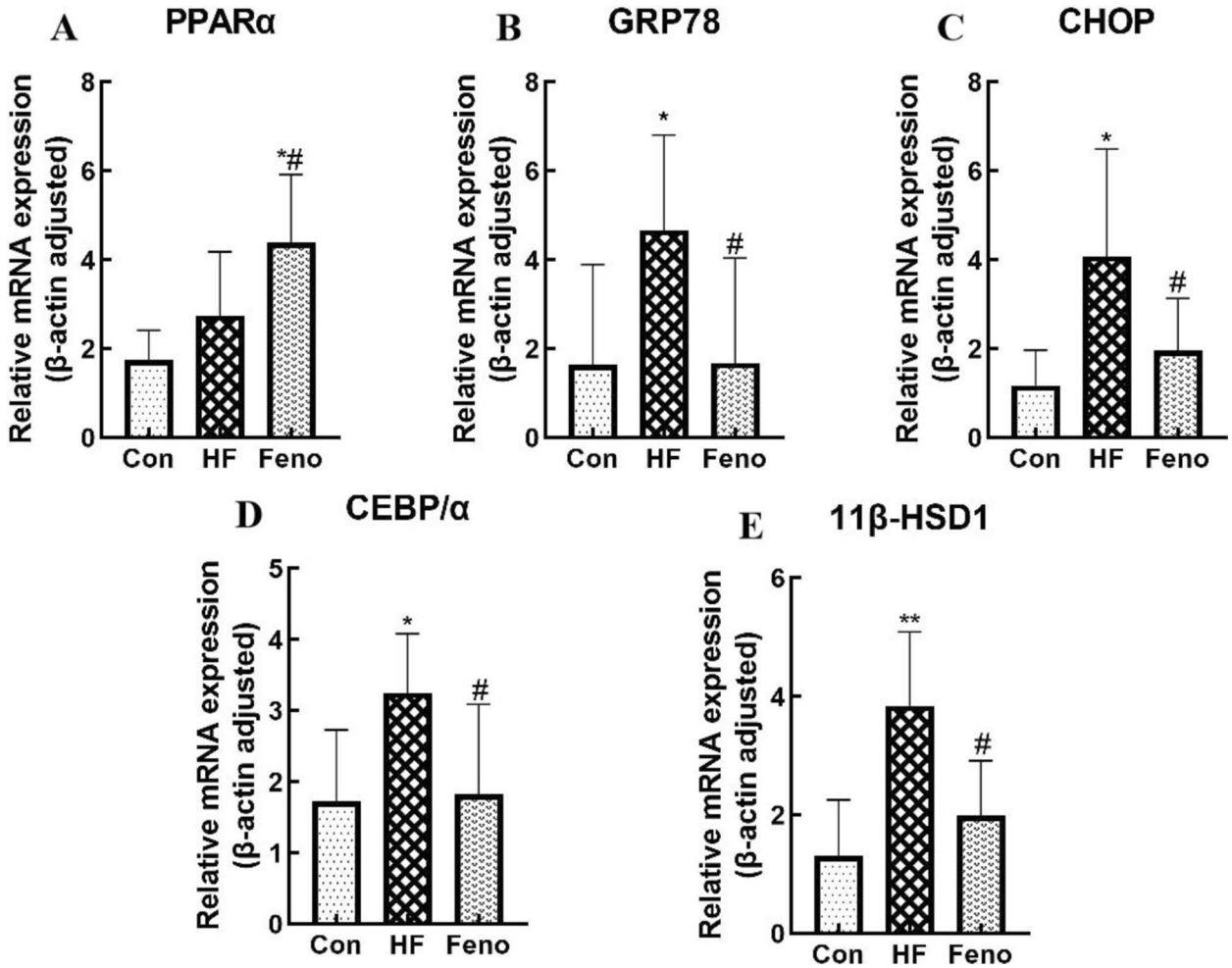

Fig. 11 Changes of mRNA expression of PPARα, ERS-CHOP-C/ EBP-α signaling pathway and 11β-HSD1 in liver of high-fat golden hamsters and effects of fenofibrate intervention. *$P < 0.05$ versus the Con group; **$P \leq 0.001$ versus the Con group; #$P < 0.05$ versus the HF group; ##$P \leq 0.001$ versus the HF group

proteins at this site, with C/EBPα playing a central role as a regulator of energy metabolism. C/EBPα is an effective transcriptional activator of 11β-HSD1 both in vivo and in vitro, further regulating intracellular GCs levels and the expression of key genes involved in glucose and lipid metabolism [39]. Vara Prasad SS et al. proposed that elevated FFA levels upregulate 11β-HSD1 expression by altering C/EBPα gene expression, thereby enhancing the local amplification of GC action [8]. Treatment with ER stress inhibitors during cell culture suppresses the production of 11β-HSD1 and cortisol [40].

Our study, based on both Western blot and RT-PCR results, confirmed that high-fat feeding in golden hamsters increases FFA levels, which, in turn, elevate markers of ERS such as GRP78 and key downstream molecules like CHOP. ERS enhances the translation of C/EBPα in liver cells, leading to increased expression of 11β-HSD1 and elevated corticosterone levels. This suggests that FFA may regulate the expression of 11β-HSD1 in the liver of high-fat-fed golden hamsters via the ERS-CHOP-C/EBPα signaling pathway (See Fig. 12).

Similar to GCs, PPARα promotes hepatic fatty acid oxidation and transport during fasting to provide energy, while it increases de novo lipogenesis during feeding to store lipids. PPARα may regulate the dynamic balance of fatty acid oxidation and synthesis in the liver according to nutritional status and circadian rhythms [41]. Fenofibrate can reduce body weight, fasting blood glucose, insulin, TC, TG, FFA, and PA levels, while increasing serum HDL-C levels [42]. In this study, high-fat feeding resulted in increased weight and elevated TC, TG, FFA, HDL-C, and LDL-C levels in golden hamsters, which were significantly higher than in the control group. After fenofibrate intervention, weight decreased, and TC, TG, LDL-C, and FFA levels decreased significantly, while HDL-C levels increased, consistent with findings reported in the literature [43].

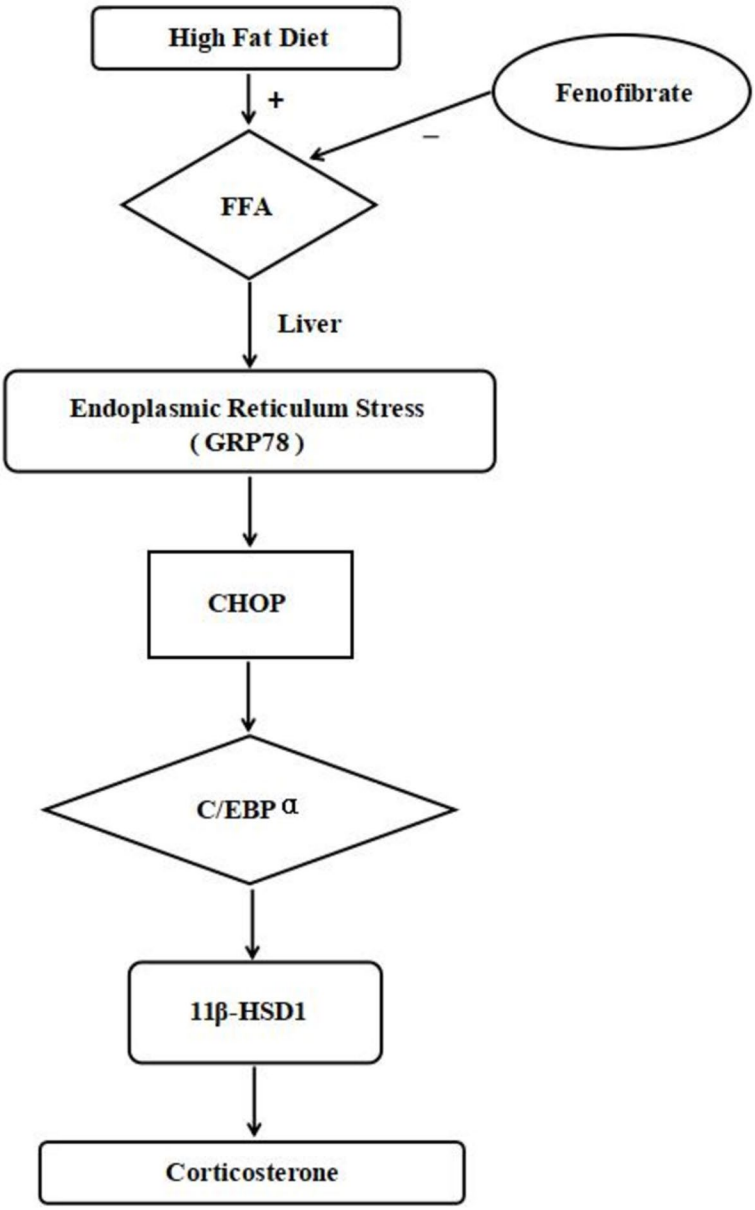

Fig.12 Free fatty acids may regulate the expression of 11β-hydroxysteroid dehydrogenase 1 in liver of high-fat fed golden hamsters through ERS-CHOP-C/ EBP-α signaling pathway

Fenofibrate significantly improved ERS and inflammation induced by high-fat diets or palmitate by increasing fatty acid β-oxidation, correcting lipid composition disorders in the ER, and improving hepatic steatosis [42, 44, 45]. PPARα gene knockout or inhibition of PPARα signaling impairs mitochondrial integrity, damages enzymes involved in fatty acid β-oxidation, and increases the expression of hepatic apoB, which affects the expression of ER calcium ATPases and induces hepatic ERS. Restoring PPARα activity can alleviate mitochondrial dysfunction and ERS, reduce systemic hypertriglyceridemia, and improve hepatic steatosis [46]. As early as 2000, Hermanowski-Vosatka A et al. showed that long-term treatment with a PPARα agonist significantly downregulated the expression and activity of 11β-HSD1 in the liver of wild-type mice, whereas PPARα knockout or treatment with a PPARα agonist for just 7 h had no effect on 11β-HSD1 levels in the liver. This was the first demonstration that PPARα agonists can influence liver GC metabolism by altering 11β-HSD1 expression [23].

Gao H et al. proposed that GCs stimulate hepatic PPARα expression at the transcriptional level via GRα, and in turn, PPARα inhibits 11β-HSD1 expression to counteract the effects of GCs. PPARα also downregulates hepatic GR mRNA and protein expression, forming a negative feedback loop [47]. In our study, fenofibrate intervention increased hepatic PPARα levels, decreased FFA levels, reduced the expression of ERS-CHOP-C/EBPα signaling pathway-related proteins, and lowered 11β-HSD1 expression and corticosterone levels in high-fat-fed golden hamsters. This further supports the hypothesis that FFAs may regulate 11β-HSD1 expression through the ERS-CHOP-C/EBPα signaling pathway (See Fig. 12), consistent with previously reported findings.

Our results provide new insights into the molecular mechanisms by which FFAs influence 11β-HSD1 expression. They also provide a basis for the use of fenofibrate in lowering local tissue 11β-HSD1 and GC levels and exploring new therapeutic targets for metabolic diseases. However, our study has some limitations, as it primarily focuses on the changes in 11β-HSD1 gene expression regulated by FFAs through the ERS-CHOP-C/EBPα signaling pathway, without further verification using gene knockout or ERS inhibitors in golden hamsters.

Conclusion

This study found that high levels of FFA lead to an increase in 11β-HSD1 and corticosterone levels in the liver of golden hamsters. After treatment with fenofibrate, both 11β-HSD1 and corticosterone levels significantly decreased. Further analysis suggests that FFA may regulate the expression of 11β-HSD1 via the ERS-CHOP-C/EBPα signaling pathway, thereby altering corticosterone levels in local tissues. These findings provide new insights into the molecular mechanism by which FFA affects 11β-HSD1 expression and explore new therapeutic targets for the prevention and treatment of metabolic diseases.

Acknowledgements

We deeply appreciate the instructors at the Clinical Medical Research Centre of Hebei General Hospital for their help with this study. We appreciate Editage (www.editage.cn) for English language editing.

Authors' contributions

Authors' contributions: D.L.: Conceptualization, Methodology, Investigation, Data curation, Writing-original draft, Visualization. P.T.: Investigation, Data curation. Y.H.: Methodology, Data curation. T.Z.: Investigation, Data curation. X.H.: Investigation. L.L.: Investigation. X.L.: Investigation. K.Z.: Investigation. C.W.: Methodology, Writing-review & editing. G.S.: Conceptualization, Resources, Writing-review & editing. All authors contributed to the article and approved the submitted version.

Funding

This study was supported by the National Natural Science Foundation of China (82170878).

Data availability

No datasets were generated or analysed during the current study.

Declarations

Ethics approval and consent to participate

The ethics committee of Hebei General Hospital approved the research protocol (approval number: 202226, approval date: 19 July 2022).

Competing interests

The authors declare no competing interests.

Author details

[1]Department of Internal Medicine, Hebei Medical University, Shijiazhuang, Hebei 050017, People's Republic of China. [2]Department of Endocrinology, Hebei General Hospital, Shijiazhuang, Hebei 050051, People's Republic of China. [3]Department of Endocrinology, Baoding First Central Hospital, Baoding, Hebei 071000, People's Republic of China. [4]Second Department of Endocrinology and Metabolism, Cangzhou Central Hospital, Cangzhou, Hebei 061001, People's Republic of China. [5]Department of Endocrinology, Harrison International Peace Hospital, Hengshui, Hebei 053000, People's Republic of China. [6]Hebei Key Laboratory of Metabolic Diseases, Hebei General Hospital, Shijiazhuang, Hebei 050051, People's Republic of China.

Received: 18 December 2024 Accepted: 1 February 2025
Published online: 07 February 2025

References

1. Esteban NV, Loughlin T, Yergey AL, Zawadzki JK, Booth JD, Winterer JC, Loriaux DL. Daily cortisol production rate in man determined by stable isotope dilution/mass spectrometry. J Clin Endocrinol Metab. 1991;72(1):39–45. https://doi.org/10.1210/jcem-72-1-39.
2. Morgan SA, Hassan-Smith ZK, Lavery GG. MECHANISMS IN ENDOCRINOLOGY: Tissue-specific activation of cortisol in Cushing's syndrome. Eur J Endocrinol. 2016;175(2):R83–9. https://doi.org/10.1530/EJE-15-1237.
3. Gathercole LL, Lavery GG, Morgan SA, Cooper MS, Sinclair AJ, Tomlinson JW, Stewart PM. 11β-Hydroxysteroid dehydrogenase 1: translational and therapeutic aspects. Endocr Rev. 2013;34(4):525–55. https://doi.org/10.1210/er.2012-1050.
4. Tomlinson JW, Walker EA, Bujalska IJ, Draper N, Lavery GG, Cooper MS, Hewison M, Stewart PM. 11beta-hydroxysteroid dehydrogenase type 1: a tissue-specific regulator of glucocorticoid response. Endocr Rev. 2004;25(5):831–66. https://doi.org/10.1210/er.2003-0031.
5. Wang JC, Gray NE, Kuo T, Harris CA. Regulation of triglyceride metabolism by glucocorticoid receptor. Cell Biosci. 2012;2(1):19. https://doi.org/10.1186/2045-3701-2-19.
6. Salehidoost R, Korbonits M. Glucose and lipid metabolism abnormalities in Cushing's syndrome. J Neuroendocrinol. 2022;34(8): e13143. https://doi.org/10.1111/jne.13143.
7. Petrus P, Rosqvist F, Edholm D, Mejhert N, Arner P, Dahlman I, Rydén M, Sundbom M, Risérus U. Saturated fatty acids in human visceral adipose tissue are associated with increased 11- β-hydroxysteroid-dehydrogenase type 1 expression. Lipids Health Dis. 2015;14:42. https://doi.org/10.1186/s12944-015-0042-1.
8. Vara Prasad SS, Jeya Kumar SS, Kumar PU, Qadri SS, Vajreswari A. Dietary fatty acid composition alters 11β-hydroxysteroid dehydrogenase type 1 gene expression in rat retroperitoneal white adipose tissue. Lipids Health Dis. 2010;9:111. https://doi.org/10.1186/1476-511X-9-111.
9. Liu Y, Xu C, Gu R, Han R, Li Z, Xu X. Endoplasmic reticulum stress in diseases. MedComm (2020). 2024;5(9):e701. https://doi.org/10.1002/mco2.701.
10. Guo W, Wong S, Xie W, Lei T, Luo Z. Palmitate modulates intracellular signaling, induces endoplasmic reticulum stress, and causes apoptosis in mouse 3T3-L1 and rat primary preadipocytes. Am J Physiol Endocrinol Metab. 2007;293(2):E576–86. https://doi.org/10.1152/ajpendo.00523.2006.
11. Fan Z, Xu L, Gao Y, Cao Y, Tian Y, Pan Z, Wei L, Chen S, Zhang X, Liu M, Ren F. The cytoplasmic-nuclear transport of DDX3X promotes immune-mediated liver injury in mice regulated by endoplasmic reticulum stress. Cell Death Dis. 2024;15(9):702. https://doi.org/10.1038/s41419-024-07076-9.
12. Hu H, Tian M, Ding C, Yu S. The C/EBP Homologous Protein (CHOP) Transcription Factor Functions in Endoplasmic Reticulum Stress-Induced Apoptosis and Microbial Infection. Front Immunol. 2019;9:3083. https://doi.org/10.3389/fimmu.2018.03083.

13. Hotamisligil GS. Endoplasmic reticulum stress and the inflammatory basis of metabolic disease. Cell. 2010;140(6):900–17. https://doi.org/10.1016/j.cell.2010.02.034.
14. Marwarha G, Claycombe K, Schommer J, Collins D, Ghribi O. Palmitate-induced Endoplasmic Reticulum stress and subsequent C/EBPα Homologous Protein activation attenuates leptin and Insulin-like growth factor 1 expression in the brain. Cell Signal. 2016;28(11):1789–805. https://doi.org/10.1016/j.cellsig.2016.08.012.
15. Wang L, Feng J, Deng Y, Yang Q, Wei Q, Ye D, Rong X, Guo J. CCAAT/Enhancer-Binding Proteins in Fibrosis: Complex Roles Beyond Conventional Understanding. Research (Wash D C). 2022;2022:9891689. https://doi.org/10.34133/2022/9891689.
16. Friedman AD. C/EBPα in normal and malignant myelopoiesis. Int J Hematol. 2015;101(4):330–41. https://doi.org/10.1007/s12185-015-1764-6.
17. Yang Y, Liu L, Naik I, Braunstein Z, Zhong J, Ren B. Transcription Factor C/EBP Homologous Protein in Health and Diseases. Front Immunol. 2017;8:1612. https://doi.org/10.3389/fimmu.2017.01612.
18. Marciniak SJ, Yun CY, Oyadomari S, Novoa I, Zhang Y, Jungreis R, Nagata K, Harding HP, Ron D. CHOP induces death by promoting protein synthesis and oxidation in the stressed endoplasmic reticulum. Genes Dev. 2004;18(24):3066–77. https://doi.org/10.1101/gad.1250704.
19. Liu Y, Zhu Y, Wang L, Li K, Du N, Pan X, Li Y, Cao R, Li B, Lin H, Song Y, Zhang Y, Wu X, Hu C, Wang Y, Liao S, Huang Y. Acid-sensitive ion channel 1a regulates TNF-α expression in LPS-induced acute lung injury via ERS-CHOP-C/EBPα signaling pathway. Mol Immunol. 2023;153:25–35. https://doi.org/10.1016/j.molimm.2022.11.007. (Epub 2022 Nov 17 PMID: 36403431).
20. Kersten S, Stienstra R. The role and regulation of the peroxisome proliferator activated receptor alpha in human liver. Biochimie. 2017;136:75–84. https://doi.org/10.1016/j.biochi.2016.12.019. (Epub 2017 Jan 8 PMID: 28077274).
21. Bernal-Mizrachi C, Weng S, Feng C, Finck BN, Knutsen RH, Leone TC, Coleman T, Mecham RP, Kelly DP, Semenkovich CF. Dexamethasone induction of hypertension and diabetes is PPAR-alpha dependent in LDL receptor-null mice. Nat Med. 2003;9(8):1069–75. https://doi.org/10.1038/nm898.
22. Echeverría F, Valenzuela R, Bustamante A, Álvarez D, Ortiz M, Espinosa A, Illesca P, Gonzalez-Mañan D, Videla LA. High-fat diet induces mouse liver steatosis with a concomitant decline in energy metabolism: attenuation by eicosapentaenoic acid (EPA) or hydroxytyrosol (HT) supplementation and the additive effects upon EPA and HT co-administration. Food Funct. 2019;10(9):6170–83. https://doi.org/10.1039/c9fo01373c.
23. Hermanowski-Vosatka A, Gerhold D, Mundt SS, Loving VA, Lu M, Chen Y, Elbrecht A, Wu M, Doebber T, Kelly L, Milot D, Guo Q, Wang PR, Ippolito M, Chao YS, Wright SD, Thieringer R. PPARalpha agonists reduce 11beta-hydroxysteroid dehydrogenase type 1 in the liver. Biochem Biophys Res Commun. 2000;279(2):330–6. https://doi.org/10.1006/bbrc.2000.3966.
24. Hu T, Lin M, Zhang D, Li M, Zhang J. A UPLC/MS/MS method for comprehensive profiling and quantification of fatty acid esters of hydroxy fatty acids in white adipose tissue. Anal Bioanal Chem. 2018;410(28):7415–28. https://doi.org/10.1007/s00216-018-1350-x.
25. Singh V, Jain M, Misra A, Khanna V, Prakash P, Malasoni R, Dwivedi AK, Dikshit M, Barthwal MK. Curcuma oil ameliorates insulin resistance & associated thrombotic complications in hamster & rat. Indian J Med Res. 2015;141(6):823–32. https://doi.org/10.4103/0971-5916.160719.PMID: 26205026;PMCID:PMC4525408.
26. Srivastava RA, He S. Anti-hyperlipidemic and insulin sensitizing activities of fenofibrate reduces aortic lipid deposition in hyperlipidemic Golden Syrian hamster. Mol Cell Biochem. 2010;345(1–2):197–206. https://doi.org/10.1007/s11010-010-0573-8.
27. Hiel S, Neyrinck AM, Rodriguez J, Pachikian BD, Bouzin C, Thissen JP, Cani PD, Bindels LB, Delzenne NM. Inulin Improves Postprandial Hypertriglyceridemia by Modulating Gene Expression in the Small Intestine. Nutrients. 2018;10(5):532. https://doi.org/10.3390/nu10050532.
28. Walker BR. Extra-adrenal regeneration of glucocorticoids by 11beta-hydroxysteroid dehydrogenase type 1: physiological regulator and pharmacological target for energy partitioning. Proc Nutr Soc. 2007;66(1):1–8. https://doi.org/10.1017/S002966510700523X.
29. Basu R, Singh RJ, Basu A, Chittilapilly EG, Johnson CM, Toffolo G, Cobelli C, Rizza RA. Splanchnic cortisol production occurs in humans: evidence for conversion of cortisone to cortisol via the 11-beta hydroxysteroid dehydrogenase (11beta-hsd) type 1 pathway. Diabetes. 2004;53(8):2051–9. https://doi.org/10.2337/diabetes.53.8.2051.
30. Yang F, Dai Y, Min C, Li X. Neonatal overfeeding induced glucocorticoid overexposure accelerates hepatic lipogenesis in male rats. Nutr Metab (Lond). 2018;15:30. https://doi.org/10.1186/s12986-018-0272-0.
31. Sieber-Ruckstuhl NS, Zini E, Osto M, Franchini M, Boretti FS, Meli ML, Sigrist B, Lutz TA, Reusch CE. Effect of hyperlipidemia on 11β-hydroxysteroid-dehydrogenase, glucocorticoid receptor, and leptin expression in insulin-sensitive tissues of cats. Domest Anim Endocrinol. 2010;39(4):222–30. https://doi.org/10.1016/j.domaniend.2010.06.003.
32. Iwasaki Y, Takayasu S, Nishiyama M, Tsugita M, Taguchi T, Asai M, Yoshida M, Kambayashi M, Hashimoto K. Is the metabolic syndrome an intracellular Cushing state? Effects of multiple humoral factors on the transcriptional activity of the hepatic glucocorticoid-activating enzyme (11beta-hydroxysteroid dehydrogenase type 1) gene. Mol Cell Endocrinol. 2008;285(1–2):10–8. https://doi.org/10.1016/j.mce.2008.01.012.
33. Li H, Sheng J, Wang J, Gao H, Yu J, Ding G, Ding N, He W, Zha J. Selective Inhibition of 11β-Hydroxysteroid Dehydrogenase Type 1 Attenuates High-Fat Diet-Induced Hepatic Steatosis in Mice. Drug Des Devel Ther. 2021;15:2309–24. https://doi.org/10.2147/DDDT.S285828.
34. Gundu C, Arruri VK, Sherkhane B, Khatri DK, Singh SB. GSK2606414 attenuates PERK/p-eIF2α/ATF4/CHOP axis and augments mitochondrial function to mitigate high glucose induced neurotoxicity in N2A cells. Curr Res Pharmacol Drug Discov. 2022;3: 100087. https://doi.org/10.1016/j.crphar.2022.100087.
35. Gupta MK, Tahrir FG, Knezevic T, White MK, Gordon J, Cheung JY, Khalili K, Feldman AM. GRP78 Interacting Partner Bag5 Responds to ER Stress and Protects Cardiomyocytes From ER Stress-Induced Apoptosis. J Cell Biochem. 2016;117(8):1813–21. https://doi.org/10.1002/jcb.25481.
36. Chikka MR, McCabe DD, Tyra HM, Rutkowski DT. C/EBP homologous protein (CHOP) contributes to suppression of metabolic genes during endoplasmic reticulum stress in the liver. J Biol Chem. 2013;288(6):4405–15. https://doi.org/10.1074/jbc.M112.432344.
37. Oyadomari S, Harding HP, Zhang Y, Oyadomari M, Ron D. Dephosphorylation of translation initiation factor 2alpha enhances glucose tolerance and attenuates hepatosteatosis in mice. Cell Metab. 2008;7(6):520–32. https://doi.org/10.1016/j.cmet.2008.04.011.
38. Wu J, Hu G, Lu Y, Zheng J, Chen J, Wang X, Zeng Y. Palmitic acid aggravates inflammation of pancreatic acinar cells by enhancing unfolded protein response induced CCAAT-enhancer-binding protein β-CCAAT-enhancer-binding protein α activation. Int J Biochem Cell Biol. 2016;79:181–93. https://doi.org/10.1016/j.biocel.2016.08.035.
39. Williams LJ, Lyons V, MacLeod I, Rajan V, Darlington GJ, Poli V, Seckl JR, Chapman KE. C/EBP regulates hepatic transcription of 11beta -hydroxysteroid dehydrogenase type 1. A novel mechanism for cross-talk between the C/EBP and glucocorticoid signaling pathways. J Biol Chem. 2000 Sep;275(39):30232–9. https://doi.org/10.1074/jbc.M001286200.
40. Lee YB, Hwang HJ, Kim E, Lim SH, Chung CH, Choi EH. Hyperglycemia-activated 11β-hydroxysteroid dehydrogenase type 1 increases endoplasmic reticulum stress and skin barrier dysfunction. Sci Rep. 2023;13(1):9206. https://doi.org/10.1038/s41598-023-36294-y.
41. Zhou S, You H, Qiu S, Yu D, Bai Y, He J, Cao H, Che Q, Guo J, Su Z. A new perspective on NAFLD: Focusing on the crosstalk between peroxisome proliferator-activated receptor alpha (PPARα) and farnesoid X receptor (FXR). Biomed Pharmacother. 2022;154: 113577. https://doi.org/10.1016/j.biopha.2022.113577.
42. Dai F, Jiang T, Bao YY, Chen GJ, Chen L, Zhang Q, Lu YX. Fenofibrate improves high-fat diet-induced and palmitate-induced endoplasmic reticulum stress and inflammation in skeletal muscle. Life Sci. 2016;157:158–67. https://doi.org/10.1016/j.lfs.2016.06.008.
43. Li X, Zheng K, Gu W, Hou X, Guan Y, Liu L, Hou L, Geng J, Song G. Serum Fibroblast Growth Factor 21 Level After an Oral Fat Tolerance Test is Related to Postprandial Free Fatty Acid Level. Diabetes Metab Syndr Obes. 2023;16:1567–76. https://doi.org/10.2147/DMSO.S410457.
44. Balakumar P, Sambathkumar R, Mahadevan N, Muhsinah AB, Alsayari A, Venkateswaramurthy N, Dhanaraj SA. Molecular targets of fenofibrate in the cardiovascular-renal axis: A unifying perspective of its pleiotropic benefits. Pharmacol Res. 2019;144:132–41. https://doi.org/10.1016/j.phrs.2019.03.025.
45. Yuan J, Mo H, Luo J, Zhao S, Liang S, Jiang Y, Zhang M. PPARα activation alleviates damage to the cytoskeleton during acute myocardial ischemia/

reperfusion in rats. Mol Med Rep. 2018;17(5):7218–26. https://doi.org/10.3892/mmr.2018.8771.
46. Su Q, Baker C, Christian P, Naples M, Tong X, Zhang K, Santha M, Adeli K. Hepatic mitochondrial and ER stress induced by defective PPARα signaling in the pathogenesis of hepatic steatosis. Am J Physiol Endocrinol Metab. 2014;306(11):E1264–73. https://doi.org/10.1152/ajpendo.00438.2013.
47. Gao H, Li Y, Chen X. Interactions between nuclear receptors glucocorticoid receptor α and peroxisome proliferator-activated receptor α form a negative feedback loop. Rev Endocr Metab Disord. 2022;23(5):893–903. https://doi.org/10.1007/s11154-022-09725-w.

Publisher's Note